

Complete break-up of the helium atom by proton and antiproton impact

Xiaoxu Guan* and Klaus Bartschat†

Department of Physics and Astronomy, Drake University, Des Moines, Iowa 50311, USA

(Dated: June 6, 2022)

We present a fully *ab initio*, non-perturbative, time-dependent approach to describe single and double ionization of helium by proton and antiproton impact. A flexible and accurate finite-element discrete-variable-representation is applied to discretize the problem on the radial grid in spherical coordinates. Good agreement with the most recent experimental data for absolute angle-integrated cross sections is obtained over a wide range of incident projectile energies between 3 keV and 6 MeV. Furthermore, angle-differential cross sections for two-electron ejection are predicted for a proton impact energy of 6 MeV. Finally, the time evaluation of the ionization process is portrayed by displaying the electron density as a function of the projectile location.

PACS numbers: 36.10.-k, 31.15.A-, 25.40.Ep, 25.43.+t

Ionization of helium by slow antiproton impact has received considerable attention in recent months, from experimentalists [1, 2] and theorists alike [3, 4]. As a fundamental, strongly correlated few-body collision system, it is at the heart of examining the reliability of the most advanced computational methods for atomic collision processes. Using antiprotons has the major advantage of eliminating the complicated charge-exchange process that is competing with single ionization in the case of proton impact.

Of particular interest regarding the validity of theoretical approaches is the low-energy region, where the projectile speed $|\mathbf{v}|$ is sufficiently slow that the Massey perturbation parameter $|Z_p|/|\mathbf{v}|$ [5], where Z_p is the charge of the projectile, is becoming larger than unity. Note that $|Z_p|/|\mathbf{v}| = 1$ for incident (anti)protons with energy $E_i \simeq 25$ keV. Consequently, perturbative treatments based on one or even a few terms of the Born series are entirely inappropriate for the problem at this and lower energies. Instead, non-perturbative treatments, either based upon the close-coupling expansion with an appropriate set of basis functions [6, 7] or the direct solution of the time-dependent Schrödinger equation (TDSE) on a numerical space-time grid [3, 4, 8] are required. The latter method is often referred to as the time-dependent close-coupling (TDCC) approach.

The interaction between the charged projectile and the target can also be viewed as a temporal ultrafast half-cycle-like pulse, which is responsible for the (multiple) ionization process of the target [9]. The full width at half maximum of such a pulse can be estimated as $2\sqrt{3}b/|v_p|$. For (anti)proton impact, this is of the order 10 attoseconds for “intermediate” energies around 100 keV. Furthermore, the peak strength of the electric field \mathcal{U}_{\max} is of the order $Z_p/|b|$. Even for (anti)protons as the lightest “heavy” particles, \mathcal{U}_{\max} is approximately two atomic units at an impact parameter $|b| \simeq 1a_0$, where $a_0 = 0.529 \times 10^{-10}$ m is the Bohr radius. This results in peak intensities of the half-cycle pulse as high as 10^{17} W/cm². Consequently, charged-ion impact presents an interesting alternative to intense laser-pulse techniques in the study of ionization processes in strong electromagnetic fields within an ultrashort time window [9].

Various experimental datasets for single and double ionization of helium by antiproton impact were published over the years. While there is generally good agreement at high incident energies, both between different experimental datasets and predictions from various theoretical models, the situation is much less clear for incident energies of 20 keV and below. Most recently, Knudsen *et al.* [1] published results for single ionization of helium by antiproton impact that differed substantially from those obtained earlier by Andersen *et al.* [10] and Hvelplund *et al.* [11]. While the recent experimental data of Knudsen *et al.* [1] were reproduced fairly well by various non-perturbative calculations [3, 6, 7], discrepancies of 15% or more still remained.

Here we report results from a fully *ab initio* numerical study of the helium break-up problem by antiproton and proton impact over a wide range of incident energies between 3 keV to 6 MeV, as well as the corresponding total and double-differential cross sections (DDCS). Our approach, whose validity is not restricted to a particular projectile energy range, thus provides a unique opportunity for studying the multiple ionization dynamics induced by charged ions from weak to strong perturbations. The configuration space of the target electrons is discretized via a finite-element discrete-variable representation (FE-DVR). This highly flexible and accurate grid-based approach combines the numerical advantages of basis-function expansions in small intervals with an easily adaptable spatial grid to account for the radial dependence of the electronic wavefunction close to and far away from the nucleus.

The dynamical response of the system is obtained by propagating the initial wavepacket, defined on the DVR gridpoints, through a recently developed time-dependent Arnoldi-Lanczos algorithm [12, 13]. The collision system is governed by the time-dependent Hamiltonian

$$\mathcal{H}(t) = -\frac{\nabla_1^2}{2} - \frac{\nabla_2^2}{2} - \frac{Z_t}{r_1} - \frac{Z_t}{r_2} + \frac{1}{|\mathbf{r}_1 - \mathbf{r}_2|} + \mathcal{U}_p(t). \quad (1)$$

The essential complexity, compared to previous work involving a spatially homogeneous laser field [12], is the rep-

representation of the two-body Coulomb interaction

$$\begin{aligned} \mathcal{U}_p(t) &= -Z_p/|\mathbf{r}_1 - \mathbf{R}(t)| - Z_p/|\mathbf{r}_2 - \mathbf{R}(t)| \\ &= -Z_p \sum_{\lambda_1 q_1} \frac{4\pi}{2\lambda_1 + 1} \frac{[r_1, R(t)]_{<}^{\lambda_1}}{[r_1, R(t)]_{>}^{\lambda_1 + 1}} Y_{\lambda_1 q_1}^*(\hat{\mathbf{r}}_1) Y_{\lambda_1 q_1}(\hat{\mathbf{R}}(t)) \\ &\quad - Z_p \sum_{\lambda_2 q_2} \frac{4\pi}{2\lambda_2 + 1} \frac{[r_2, R(t)]_{<}^{\lambda_2}}{[r_2, R(t)]_{>}^{\lambda_2 + 1}} Y_{\lambda_2 q_2}^*(\hat{\mathbf{r}}_2) Y_{\lambda_2 q_2}(\hat{\mathbf{R}}(t)) \quad (2) \end{aligned}$$

between the projectile and the target. Here \mathbf{r}_1 and \mathbf{r}_2 are the coordinates of the two helium electrons, $\mathbf{R}(t)$ is the coordinate of the projectile, and $[x, y]_{<(>)} \equiv \min(\max)\{x, y\}$. All these coordinates are defined relative to the He^{2+} ion, which is fixed at the origin.

We use a straight-line trajectory $\mathbf{R}(t) = \mathbf{b} + (\mathbf{d}_0 - \mathbf{v}t)$ for the incident projectile starting at \mathbf{d}_0 at an impact parameter \mathbf{b} . This is the only physical approximation made in our treatment. It should be sufficiently accurate even

at a projectile energy as low as 3 keV, which is the lowest energy considered in this work. At this energy and $|\mathbf{b}| \simeq 1 a_0$, which is the impact-parameter regime with the largest contribution to the cross sections, the scattering angle in the laboratory system is estimated to be merely 1° . This results in a small relative momentum transfer $|\mathbf{q}|/|\mathbf{P}_i|$ of 1.8%, where \mathbf{P}_i is the projectile's initial momentum.

As a result of using a classical trajectory for the projectile, the total angular momentum L , magnetic quantum number M , and parity Π of the collision system are no longer conserved quantities that could be taken advantage of in a fully quantal partial-wave expansion. However, there is still one conserved quantity, namely the reflection symmetry of the electronic wavefunction with respect to the collision plane. The latter is defined by the trajectory of the incident projectile and the impact parameter \mathbf{b} .

We explicitly build this reflection symmetry into our FE-DVR wavefunction by writing

$$\begin{aligned} \Psi(\mathbf{r}_1, \mathbf{r}_2, t) &= \sum_{LM, l_1 l_2} \sum_{j < i} \left[f_i(r_1) f_j(r_2) C_{l_1 l_2 LM}^{ij}(t) + (-1)^{l_1 + l_2 - L} f_j(r_1) f_i(r_2) C_{l_2 l_1 LM}^{ij}(t) \right] \mathcal{G}_{l_1 l_2}^{LM}(\hat{\mathbf{r}}_1, \hat{\mathbf{r}}_2) \\ &\quad + \sum_{LM, l_1 \leq l_2} \sum_i f_i(r_1) f_i(r_2) C_{l_1 l_2 LM}^{ii}(t) \frac{1}{1 + \delta_{l_1 l_2}} \left(\mathcal{G}_{l_1 l_2}^{LM}(\hat{\mathbf{r}}_1, \hat{\mathbf{r}}_2) + (-1)^{l_1 + l_2 - L} \mathcal{G}_{l_2 l_1}^{LM}(\hat{\mathbf{r}}_1, \hat{\mathbf{r}}_2) \right). \quad (3) \end{aligned}$$

Instead of ordinary coupled spherical harmonics $\mathcal{Y}_{l_1 l_2}^{LM}(\hat{\mathbf{r}}_1, \hat{\mathbf{r}}_2)$, we introduced the angular basis

$$\mathcal{G}_{l_1 l_2}^{LM}(\hat{\mathbf{r}}_1, \hat{\mathbf{r}}_2) \equiv \sqrt{\frac{2}{1 + \delta_{l_1 l_2}}} \text{Re} \left[\mathcal{Y}_{l_1 l_2}^{LM}(\hat{\mathbf{r}}_1, \hat{\mathbf{r}}_2) \right]. \quad (4)$$

These basis functions are normalized according to $\langle \mathcal{G}_{l_1 l_2}^{LM} | \mathcal{G}_{l_1' l_2'}^{L' M'} \rangle = \delta_{l_1 l_1'} \delta_{l_2 l_2'} \delta_{LL'} \delta_{MM'}$. Using the reflection symmetry relates the wavefunctions for the magnetic quantum numbers M and $-M$, in the same way as it does for electron-impact excitation and coplanar ionization and ionization-excitation processes [14]. Consequently, we only need to include $M \geq 0$ in Eq. (3) and thus the size of the problem is reduced to nearly half of what it would be without adopting the above symmetry. Taking advantage of the reflection symmetry, we use 55 angular partial waves generated by setting $(l_1, l_2, L, M)_{\max} = (3, 3, 3, 3)$ to expand the wave function in Eq. (3). This is equivalent to the 101 partial waves used in Ref. [3].

To calculate the angle- and energy-integrated cross sections, 399 DVR grid points were set up in a spatial box of $r_{\max} = 80 a_0$, while a smaller step size and 799 points were employed for the DDOS. We also extended the box size to $160 a_0$ in this case to ensure converged results.

The total cross section (angle- and energy-integrated) is obtained as

$$\sigma(E_i) = 2\pi \int_0^{+\infty} P(b, E_i) b db, \quad (5)$$

where $P(b, E_i) = \int |\langle \Phi_{k_1 k_2} | \Psi(t) \rangle|^2 dk_1 dk_2$ represents the probability for single or double ionization at fixed values of $|\mathbf{b}|$ and E_i . Figure 1 exhibits our results for single ionization of helium by antiproton impact for projectile energies between 3 keV and 5 MeV. In the theoretically most difficult low-energy regime, we obtain excellent agreement with the most recent experimental data of Knudsen *et al.* [1]. For projectile energies of 20 keV and above, our results are slightly lower than those of Foster *et al.* [3] and thus in better agreement with experiment. On the other hand, most experimental data near the cross section maximum around 100 keV and beyond lie above both our results and those of Foster *et al.* Having performed extensive convergence checks, we are confident in the numerical accuracy of our predictions and currently have no explanation for the remaining discrepancies.

Figure 2 depicts the corresponding results for the double ionization process. Although the size of the experimental error bars [2] is substantial and thus limits the meaning of comparing the absolute numbers between theory and experiment, we note that our results are in excellent agreement with those of Foster *et al.* [3] in the limited range of projectile energies where their data are available.

To gain further insight into the dependence of the joint two-electron response on the sign of the projectile charge, we show in the left panel of Fig. 3 an example for 100 keV antiproton impact on helium at an impact parameter of $0.5 a_0$, while the right panel shows the corresponding results for proton impact. We first note that not much hap-

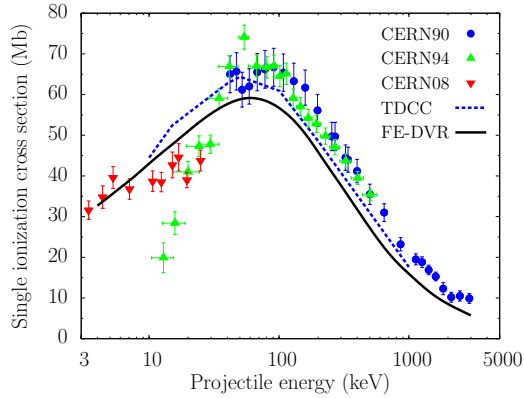


FIG. 1: (Color online) Cross section for single ionization of helium by antiproton impact. Experimental data obtained at CERN by Andersen *et al.* [10] (CERN90), Hvelplund *et al.* [11] (CERN94), and Knudsen *et al.* [1] (CERN08) are compared with TDCC [3] and the present FE-DVR predictions.

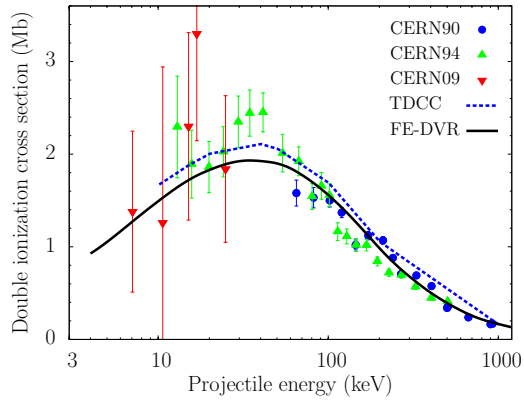


FIG. 2: (Color online) Cross section for double ionization of helium by antiproton impact. The experimental data obtained at CERN by Andersen *et al.* [10] (CERN90), Hvelplund *et al.* [11] (CERN94), and Knudsen *et al.* [2] (CERN09) are compared with TDCC [3] and the present FE-DVR predictions.

pens until the projectile is already $10 a_0$ passed the target (top panels). For this case, and also a little later when the projectile is $20 a_0$ behind the target (center panels), the radial electron densities show a substantial double-ionization component, whose signature is a significant density at large values of both r_1 and r_2 . The most energetic electrons have moved to about 25 and $50 a_0$, respectively. Finally, when the projectile is $40 a_0$ beyond the target (bottom panels), we see the characteristics of both double and single (characterized by significant densities when only r_1 or r_2 is large) ionization processes developing. By this stage, the most energetic electrons have moved as far away as $100 a_0$ from the He^{2+} center. When comparing the electron densities for the two projectile charges, we recall that the antiproton cannot capture any of the electrons and in fact pushes them away, whereas the capture channel may be important for proton impact. While the single-ionization signals for the two projectiles resemble each other, the major differ-

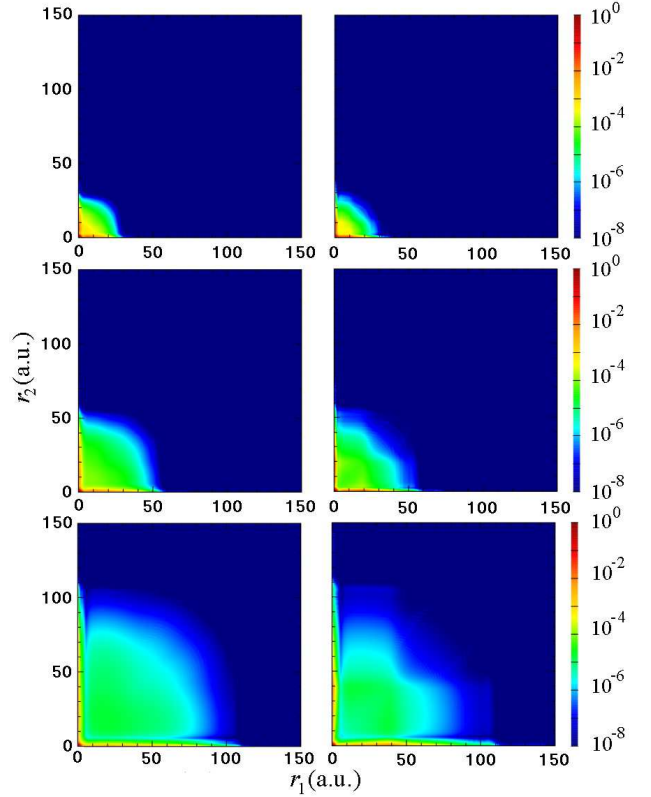


FIG. 3: (Color online) Radial electron density after antiproton (left panels) and proton (right panels) impact on helium at an energy of 100 keV for an impact parameter of $0.5 a_0$. Starting from an initial distance of $-50 a_0$, the positions of the projectile shown in the snapshots, from top to bottom, are $+10$, $+20$, and $+40 a_0$ relative to the center of the target, respectively.

ence between the results for the two projectiles occurs in the double-ionization region of $r_1 \approx r_2$. Apparently the proton is trying to attract at least one electron and hence causes a reduction in the probability for both electrons moving out with the same speed.

In order to portray the two-electron emission in a more quantitative way, it is important to consider angle-resolved cross sections, e.g., the DDCS for two-electron ejection without observing the electrons' individual energies. This particular DDCS is obtained as

$$\frac{d^2\sigma}{d\hat{\mathbf{k}}_1 d\hat{\mathbf{k}}_2} = 2\pi \int_0^{+\infty} b db \int_0^{+\infty} dk_1 \int_0^{+\infty} dk_2 \left| \sum_{LM, l_1 l_2} (-i)^{l_1 + l_2} \times e^{i(\sigma_{l_1} + \sigma_{l_2})} \mathcal{F}_{b, l_1 l_2}^{LM}(k_1, k_2) \mathcal{G}_{l_1 l_2}^{LM}(\hat{\mathbf{k}}_1, \hat{\mathbf{k}}_2) \right|^2, \quad (6)$$

where σ_l denotes the Coulomb phase and $\mathcal{F}_{b, l_1 l_2}^{LM}(k_1, k_2)$ is the partial-wave amplitude in momentum space.

Figure 4 exhibits such DDCS results for proton impact double ionization of helium for an incident energy of 6 MeV . The results are for the coplanar geometry, where the momentum transfer and the momentum vectors of the two ejected electrons all lie in the same plane. We compare our FE-DVR predictions for cuts with fixed values of

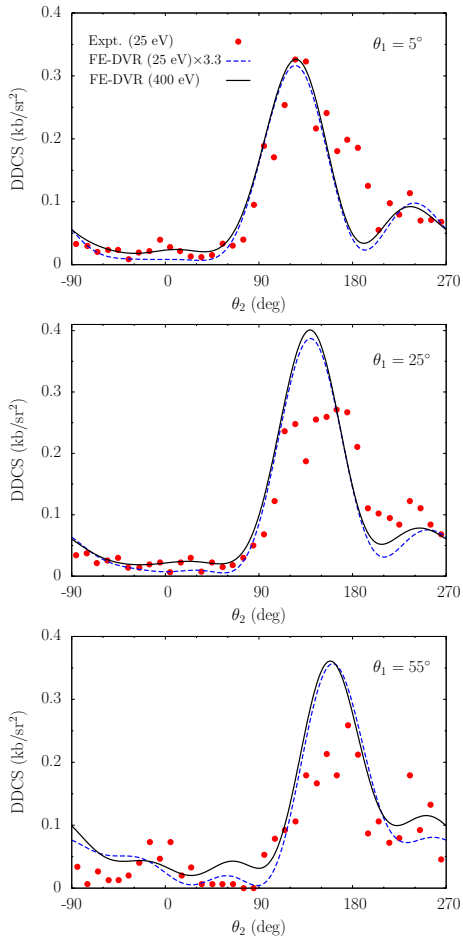


FIG. 4: (Color online) DDCS for proton impact double ionization of helium for an incident energy of 6 MeV, a fixed detection angle θ_1 for one of the electrons, and a variable detection angle θ_2 for the second electron. The experimental measurements of Refs. [15, 16] were normalized to the converged DDCS at the large peak for $\theta_1 = 5^\circ$.

θ_1 that were generated by Foster *et al.* [4] from the original experimental data of Fischer *et al.* [15] after the analysis by Schulz *et al.* [16].

Note that only ejected electrons with energies up to 25 eV were observed experimentally, while converged results for the DDCS defined in Eq. (6) require energies up to $\simeq 400$ eV to be counted in this case. Although the measured signal thus only corresponds to about one third of the converged DDCS, we see that the shape of the DDCS is essentially determined even with the cutoff at 25 eV.

We see good agreement with the experimental data and clearly reproduce the systematic shift of the large peak to the right with increasing values of θ_1 . Furthermore, the angle between θ_1 and the maximum in the DDCS as a function of θ_2 decreases slowly from about 120° for $\theta_1 = 5^\circ$ to about 100° for $\theta_1 = 55^\circ$. Similar results were published by Foster *et al.* [4], but both the graphical presentation and the theoretical magnitudes given in Fig. 2 of their paper contain errors [17].

Finally, we obtained values of 3.54 and 8.97×10^{-3} Mb, respectively, for the total cross sections for single and dou-

ble ionization. Not surprisingly for such a high projectile energy, their ratio of $\simeq 400$ is consistent with what one would expect from the shake-off mechanism.

In summary, we have investigated the complete break-up problem of helium by proton and antiproton impact by using a time-dependent non-perturbative FE-DVR approach. This is a prime example of a highly correlated four-body Coulomb process, whose description remains a major theoretical and computational challenge. Generally good agreement with the latest sets of experimental data for both integrated and differential cross sections was obtained. At lower projectile energies (< 20 keV), our antiproton results clearly show that the cross section for double ionization decreases with decreasing projectile energy. For the angle-resolved DDCS presented here, converged results require to account for contributions from ejected electrons with energies of several hundred eV, whereas the angular dependence is essentially established by low-energy electrons with energies of less than $\simeq 25$ eV.

We thank Prof. Helge Knudsen for sending us experimental data in numerical form and helpful discussions and Dr. James Colgan for clarifying problems with Ref. [4]. This work was supported by the NSF under grant PHY-0757755 and supercomputer resources through the Tera-grid allocation TG-PHY090031.

* Electronic address: xiaoxu.guan@drake.edu

† Electronic address: klaus.bartschat@drake.edu

- [1] H. Knudsen *et al.*, Phys. Rev. Lett. **101**, 043201 (2008).
- [2] H. Knudsen *et al.*, Nucl. Instrum. Methods Phys. Res. B **267**, 244 (2009).
- [3] M. Foster, J. Colgan, and M. S. Pindzola, Phys. Rev. Lett. **100**, 033201 (2008).
- [4] M. Foster, J. Colgan, and M. S. Pindzola, J. Phys. B **41**, 111002 (2008).
- [5] J. H. McGuire, in *Electron Correlation Dynamics in Atomic Collisions* (Cambridge University Press, 1997).
- [6] T. Kirchner *et al.*, J. Phys. B **35**, 925 (2003).
- [7] M. Keim *et al.*, Phys. Rev. **67**, 062711 (2003).
- [8] D. R. Schultz and P. S. Krstic, Phys. Rev. A **66**, 022717 (2003).
- [9] *Many-Particle Quantum Dynamics in Atomic and Molecular Fragmentation*, eds. J. Ullrich and V. Shevelko (Springer-Verlag, Berlin Heidelberg 2003); see Ch. 21.
- [10] L. H. Andersen *et al.*, Phys. Rev. A **41**, 6536 (1990).
- [11] P. Hvelplund *et al.*, J. Phys. B. **27**, 925 (1994).
- [12] X. Guan, K. Bartschat, and B. I. Schneider, Phys. Rev. A **77**, 043421 (2008).
- [13] X. Guan, *et al.*, Comput. Phys. Comm. (in press, 2009); see <http://dx.doi.org/10.1016/j.cpc.2009.03.005>.
- [14] N. Andersen and K. Bartschat, *Polarization, Alignment, and Orientation in Atomic Collisions* (New York: Springer 2001).
- [15] D. Fischer *et al.*, Phys. Rev. Lett. **90**, 243201 (2003).
- [16] M. Schulz *et al.*, J. Phys. B **38**, 1363 (2005).
- [17] J. Colgan, private communication (2009). An erratum to Ref. [4] is currently in preparation.